heritage

MDPI

Article

X-ray Fluorescence Spectroscopy of Picrolite Raw Material on Cyprus

Theodora Moutsiou [1,2,3,*], Demetrios Ioannides [1], Andreas Charalambous [1], Sebastian Schöder [4], Sam M. Webb [5], Mathieu Thoury [6], Vasiliki Kassianidou [1], Zomenia Zomeni [7] and Christian Reepmeyer [1,2,3]

1 Archaeological Research Unit, University of Cyprus, P.O. Box 20537, Nicosia 1678, Cyprus; ioannidis.dimtrios@ucy.ac.cy (D.I.); charalambous.c.andreas1@ucy.ac.cy (A.C.); v.kassianidou@ucy.ac.cy (V.K.); christian.reepmeyer@jcu.edu.au (C.R.)
2 ARC Centre of Excellence for Australian Biodiversity and Heritage, College of Arts, Society and Education, James Cook University, P.O. Box 6811, Cairns, QLD 4870, Australia
3 Department of Archaeology, Max Planck Institute for the Science of Human History, Kahlaische Strasse 10, D-07745 Jena, Germany
4 PUMA Beamline, Synchrotron SOLEIL, Saint-Aubin BP48, F-91192 Gif-sur-Yvette, France; sebastian.schoeder@synchrotron-soleil.fr
5 SLAC National Accelerator Laboratory, Stanford University, 2575 Sand Hill Rd., Mailstop 0069, Menlo Park, CA 94025, USA; samwebb@slac.stanford.edu
6 IPANEMA, Synchrotron SOLEIL, Saint-Aubin BP48, F-91192 Gif-sur-Yvette, France; mathieu.thoury@synchrotron-soleil.fr
7 Geological Survey Department, P.O. Box 24543, Lefkosia 1301, Cyprus; zzomeni@gsd.moa.gov.cy
* Correspondence: tmouts01@ucy.ac.cy

check for updates

Citation: Moutsiou, T.; Ioannides, D.; Charalambous, A.; Schöder, S.; Webb, S.M.; Thoury, M.; Kassianidou, V.; Zomeni, Z.; Reepmeyer, C. X-ray Fluorescence Spectroscopy of Picrolite Raw Material on Cyprus. *Heritage* **2022**, *5*, 664–676. https://doi.org/10.3390/heritage5020037

Academic Editors: Nikolaos Laskaris, Georgios Mastrotheodoros, Maria Kaparou and Artemios Oikonomou

Received: 27 February 2022
Accepted: 28 March 2022
Published: 29 March 2022

Publisher's Note: MDPI stays neutral with regard to jurisdictional claims in published maps and institutional affiliations.

Abstract: Picrolite artefacts comprise some of the most distinctive material remains in the prehistory of the island of Cyprus, in the Eastern Mediterranean. Picrolite exploitation dates from at least 12,000 years ago for the manufacture of personal ornaments and items with a symbolic function. It is commonly assumed that picrolite nodules were collected in secondary deposits on an ad hoc basis. This narrative, however, ignores the fact that picrolite carriers can only be found in very specific locations on the island, discrete from each other. Here we report initial outcomes of the application of handheld portable X-ray fluorescence (HHpXRF) and synchrotron-based X-ray fluorescence spectroscopy (SR-μXRF) to the analysis of picrolite raw materials performed at the newly opened PUMA beamline of the SOLEIL Synchrotron Radiation Facility. Our work refines the basic characteristics of the elemental constituents of the picrolite raw material and highlights key micro-structural differences between two distinct source regions on the Troodos Massif in western Cyprus. Picrolite source characterisation is expected to contribute significant new knowledge to the study of rare raw material consumption, prehistoric social organisation, networking and possible long-distance exchange of this idiosyncratic raw material within and beyond the island's geographic boundaries.

Keywords: picrolite; X-ray fluorescence; synchrotron microspectroscopy; sourcing; Cyprus

1. Introduction

Picrolite Use in Cypriot Prehistory

Anthropomorphic figurines in the shape of cruciforms dating to the fourth millennium BC are the hallmark of the use of picrolite in Cypriot prehistory [1–3]. Although these striking artefacts mark the epitome of consumption of picrolite on the island, the use of this raw material in the manufacture of objects, such as ornaments, can be dated to the earliest human presence on Cyprus (Figure 1). Picrolite artefacts, albeit in small quantities, have been documented from Akrotiri *Aetokremnos* [4] on the southern coast of Cyprus from stratigraphic contexts dating to ca. 12 kyr (~11,000 cal BC). The assemblage comprises six picrolite objects: one bead, three pendants and two small pebbles, probably pendant preforms.

Figure 1. Picrolite artefacts from the island of Cyprus (from Akrotiri *Aetokremmos*, Krittou Marottou *Ais Giorkis* and Kholetria *Ortos*).

The use of picrolite (Figure 2) has been subsequently well attested in Aceramic Neolithic (8900–5300 cal BC) sites, where the raw material was used to carve a range of forms and types of objects: beads, rings, dress-pins, small vessels or containers as well as items whose function remains unknown, such as the "thimbles" from Kritou Marottou *Ais Giorkis* [5]. Occasionally, picrolite reaches archaeological sites in unmodified form, indicating the working of raw materials in settlement sites. Such occurrences are documented across the island, for example in Ayia Varvara *Asprokremnos* and Khirokitia *Vouni*. In the Late Neolithic, picrolite use was less common and the forms carved were less elaborate [6]. Picrolite exploitation was abundant during the Chalcolithic, when the highly distinctive cruciform figurines were made. It was during this time that new carving techniques and a substantial extension in morphology and stylistic repertoires occurred [6].

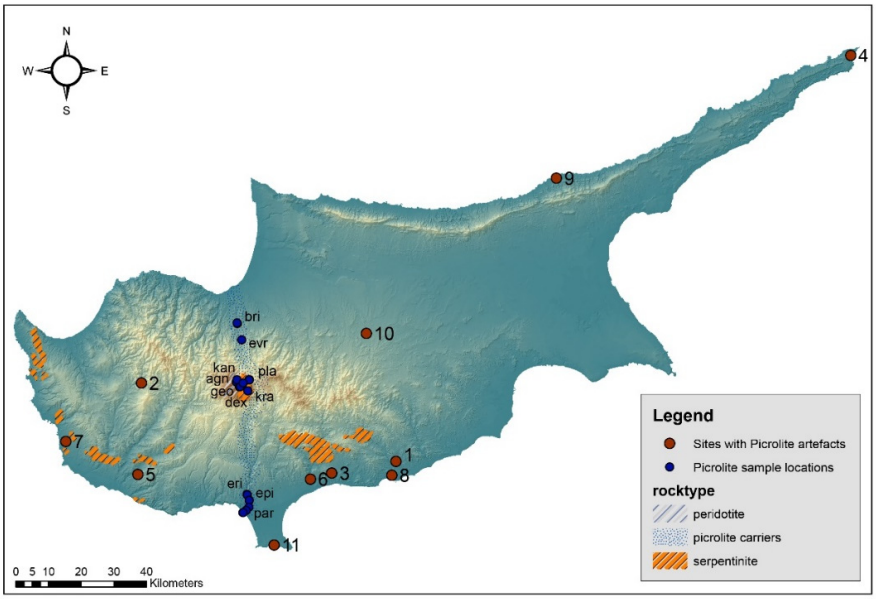

Figure 2. The map depicts the main picrolite carriers (including peridotite and serpentinite outcrops with thin picrolite veins) on Cyprus. Blue dots indicate picrolite sample locations, while red dots show Epipalaeolithic and Aceramic Neolithic archaeological sites with picrolite artefacts (1 = Khirokitia *Vouni*, 2 = Kritou Marottou *Ais Giorkis*, 3 = Ayios Tychonas *Klimonas*, 4 = Apostolos Andreas *Kastros*, 5 = Kholetria *Ortos*, 6 = Parekklisia *Shillourokambos*, 7 = Kissonerga *Mylouthkia*, 8 = Kalavasos *Tenta*, 9 = Akanthou *Arkosyko*, 10 = Ayia Varvara *Asprokremmos*, 11 = Akrotiri *Aetokremmos*).

Despite its long history of use and the high value [7] picrolite has enjoyed throughout Cypriot prehistory, major questions regarding its acquisition patterns, circulation ranges and social consumption remain unanswered. The main reason for this research gap is the lack of data and understanding of the raw material and its sources that would enable artefact provenance in a precise, accurate and systematic way. To date, little attention has been paid to determining the elemental composition of picrolite raw material and, crucially, the geochemical signatures of the various picrolite outcrops that occur on the island. Applying high-resolution geochemical analysis, we expect to be able to achieve elemental discrimination between distinct geological sources/subsources of picrolite. In doing so, we would be able to contribute significant new data in the study of Cypriot prehistoric heritage and open up new enquiries regarding the role of the island in regional interactions within the Eastern Mediterranean.

Although stone has rarely been the subject of synchrotron radiation (SR), significant outcomes can be achieved by the application of SR on this material category as well [8–13]. For example, Bernardini et al. [14] used SR-FTIR spectroscopy to analyse a set of serpentinite polished shaft-hole axes dating to the transition from the Neolithic to the Copper Age in the Caput Adriae region (northeastern Italy, central and western Slovenia and northwestern Croatia). They were able to determine raw material chemical composition and used this information to locate the primary sources of the serpentinite raw materials. Considering the success of third-generation SR-based methods in supporting provenance issues in the field of cultural heritage, this study applied SR-μXRF on picrolite raw material samples aimed at achieving source discrimination/provenance by refining the chemical composition of picrolite and defining micro-structures that may not have been identified through the bulk geochemistry analysis by HHpXRF. Even though advanced SR methods are not the first line of analytical techniques to be used in archaeological sciences, it is expected that its outcomes can be used to inform/guide benchtop or portable methods (such as HHpXRF) that do not have the spatial or energy resolution of SR-based techniques. When combined, these techniques can, subsequently, be used to rapidly distinguish a large corpus of archaeological and cultural heritage materials.

2. Background

2.1. Picrolite Raw Material

Picrolite is a soft, green massive, banded or crudely fibrous metamorphic rock with a hardness of 3.5, a waxy feel and a conchoidal to subconchoidal fracture (massive), whilst crudely fibrous varieties splinter easily [15]. Picrolite is the product of hydrothermal alternation of ultrabasic rocks, consisting of the serpentine minerals lizardite, chrysotile and antigorite, or any combination of these (for a discussion on serpentine mineral classification see [16,17]). The Cypriot variant contains predominantly lizardite and/or chrysotile with little or no significant proportions of antigorite. While serpentine $(Mg, Fe, Ni, Mn, Zn)_{2\text{-}3}(Si, Al, Fe)_2O_5(OH)_4$ mineral deposits are well documented around the globe, picrolite itself is much less frequently encountered in a geological setting, e.g., [18].

In Cyprus, primary sources (seams) of good quality picrolite occur in the Troodos Mountain Range and specifically east of the Mount Olympus summit at an elevation of about 1400 m. Here picrolite is found in veins within seprentinised harzburgite; based on geological observations it appears that serpentisation took place in situ, possibly after its emplacement with little post-alteration penetrative deformation. Joints and fractures were filled by chrysotile and picrolite and remained intact [19] p. 132. Picrolite veins, varying in thickness from a few millimetres to a few centimetres and ranging in colour from light blue-green to dark olive-green (GY7/10 light greenish grey to G6/5 greenish grey of the Munsell Color Chart), can extend for several meters on Troodos' north and south slopes. The two main rivers—namely the Kouris and Karkotis Rivers—that drain the Troodos Massif erode picrolite material, depositing it in pebble form on the north and south sides of Troodos all the way to the sea. Serpentinite outcrops are also noted in the Limassol Forest area, Akamas Peninsula, Mavrokolymbos and Diarizos and in other small serpentine

bodies within the Mamonia Complex (Figures 2 and 3). In these instances, the outcrops are heavily deformed and sheared in such a way that no usable vein material was produced. Although picrolite veins are present, these are rarely more than a few millimetres thick and, thus, unlikely to have been used by prehistoric people.

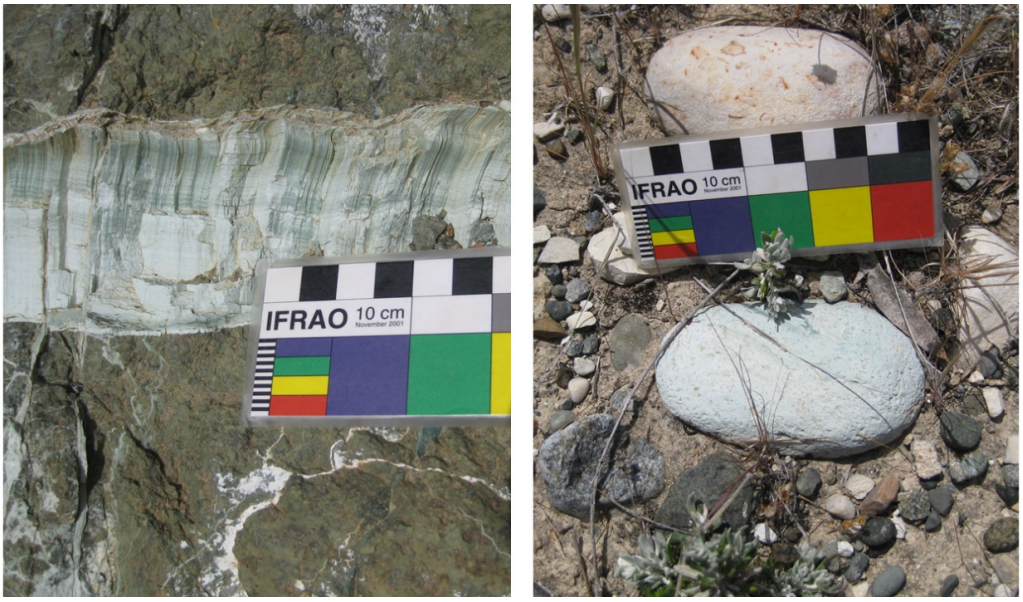

Figure 3. Picrolite in primary exposures (veins) and in secondary deposition (river pebbles).

2.2. Previous Analytical Studies on Cypriot Picrolite

Costas Manglis in [20] p. 441 was the first geologist who identified picrolite in archaeological contexts. Nevertheless, Xenophontos was the first researcher to analytically investigate Cypriot picrolite [15,19] and his work, conducted thirty years ago, remains the definitive study on picrolite raw material. Xenophontos applied neutron activation analysis (NAA) and X-ray diffraction analysis (XRD) to determine its basic mineralogical and geochemical characteristics [19]. For that he used thin sections from partly worked and unworked waterworn picrolite pebbles found at the Aceramic Neolithic site of Kholetria *Ortos* [21] and geological samples from the two main picrolite carriers, Kouris and Karkotis Rivers. He further subdivided the picrolite raw material into three different textural types see [19] (pp. 128–129), although no clear distinctions were made between source localities.

The new knowledge resulting from Xenophontos' work had a direct and long-lasting impact on the archaeology of Cyprus. Prior to his work, Archaeological artefacts made of green stones and recovered from multiple archaeological contexts across the island were invariably identified as 'steatite' [15]. Xenophontos demonstrated the inadequacy of such broad-stroke characterisations of raw materials based on purely visual features and documented the inclusion of picrolite in the raw material repertoire exploited by prehistoric populations on Cyprus. However, despite the important change in terminology and raw material association, little effort has since been placed in understanding picrolite exploitation in Cypriot prehistory. The consumption of picrolite is commonly interpreted as an expedient phenomenon, whereby the raw material was collected in pebble form from secondary deposits (riverbeds) rather than being quarried from in situ seams in upland locations (e.g., [6] but see also [22]). Although this may on occasion be the case, for example a cache of 25 picrolite pebbles is known from Khirokitia [pers. obs.], the assumption that all archaeological material derives exclusively from the nearest secondary deposits needs to be tested. This is particularly important considering that multiple picrolite carriers occur in various distinct localities across the island. Delineating primary picrolite outcrops, their geochemistry and potential division into distinct geochemical units is likely to elucidate

distinct acquisition and circulation patterns with important implications for the social organisation of prehistoric communities.

3. Materials and Methods

3.1. Picrolite Geological Samples

Picrolite geological samples and in situ locales were initially analysed to collect elemental information (Table 1). Two surveys were conducted targeting primary outcrops exposed at locations north and south of the Troodos summit, followed by further analyses of secondary deposits at multiple localities along the two main rivers carrying picrolite (Figure 2). With regards to the northern carrier, access to the sea was not possible, as the area is currently outside the effective control of the Republic of Cyprus. We did, however, sample material from as close to the northern coast/river mouth as possible. Selected samples include primary deposits on the Mount Olympus peak of the Troodos Mountain Range, and secondary locales along the two main carriers of Troodos, namely Kouris (south) and Karkotis (north) Rivers. Serpentinite deposits with occasional picrolite exposures were noted elsewhere, for example in Limassol Forest, but no samples were collected from those locales since picrolite veins when they occur are of a size too small/thin to have been used in antiquity.

Table 1. Picrolite geological samples from primary and secondary deposits from Cyprus analysed with HHpXRF and SR-μXRF at the PUMA beamline at SOLEIL. Samples with multiple interesting features underwent multiple analyses to capture the variability (see samples with asterisks *).

Source	Sample	Area	Source	Sample	Area
north	agn_120.1	square	south	dex_110.16	transect
north	agn_118.2	transect	south (secondary)	epi3_103.2	square
north	agn_118.4	square	south (secondary)	epi3_103.1	rectangular
north	agn_119.2	square	south (secondary)	epi8_105.3	square
north	agn_119.4	transect	south (secondary)	epi8_105.4 *	overview
north	agn_120.2	square	south (secondary)	epi8_105.4	overview
north	agn_120.4	transect	south (secondary)	epi8_105.4	transect
north (secondary)	bri1_100.1	square	south (secondary)	epi8_105.4	vertical lines
north (secondary)	bri1_100.2	transect	south (secondary)	eri6_104.1	square
north (secondary)	bri1_100.3	square	south (secondary)	eri6_104.4	square
north (secondary)	bri2_101.1	transect	south (secondary)	eri7_107.1 *	square
north (secondary)	bri2_102.2	square	south (secondary)	eri7_107.1	square2
north (secondary)	evr_102.1	square	south	kra_114.12	transect
north (secondary)	evr_102.2	transect	south	kra_114.13	square
north	kan_117.4	transect	south	lei_111.14	transect
			south (secondary)	par_106.4 *	square
			south (secondary)	par_106.4	square
			south (secondary)	par_106.4	square
			south	pla1_115.10	transect
			south	pla2_116.4	square
			south	pyl_112.8	transect

3.2. Sample Preparation

The samples were initially cleaned from surface contamination and sectioned to create flat surfaces for HHpXRF analysis in the lab. Analyses were conducted on clean, fresh sectioned surfaces. For SR analysis, petrographic thin sections of picrolite geological samples were prepared. The samples were mounted on quartz glass slides to minimise contamination. Evaluating the preliminary results from our earlier HHpXRF work, the 30 most promising samples were selected for additional synchrotron analysis. For comparative purposes, 15 samples from each region, i.e., north versus south, accounting for different localities across each of the picrolite zones/carriers, were chosen. Figure 2 portrays known

picrolite deposits in southwest Cyprus and locations of sample collection, highlighting collection points in the context of this study.

3.3. Handheld Portable XRF (HHpXRF)

A handheld portable X-ray fluorescence (HHpXRF, Innov-X delta, now Olympus) spectrometer was used for the chemical analysis of multiple spots/areas at selected outcrops. The specific instrument is equipped with a 4 W, 50 kV tantalum anode X-ray tube and a high-performance silicon drift detector (SDD) with a resolution of 153–155 eV (Mo-Ka). An Al filter (standard) with eight filter positions (automatic filtering) was used. The applied analytical mode was Mining Plus. For this mode, beam 1 (40 kV) determines the heavier elements Ti, V, Cr, Mn, Fe, Co, Ni, Cu, Zn, As, Zr, Mo, Pd, Ag, Cd, Sn, Sb, Hf, Ta, W, Pt, Au, Pb and Bi while beam 2 (10 kV) is used for the determination of Mg, Al, Si, P, S, Cl, K and Ca (atomic numbers: minimum 12–maximum 83). Freshly cut sections were analysed three to five times per sample. The time of analysis was 60 s. The beam size was 10 mm. In total 150 analyses were conducted on primary and secondary picrolite deposits. All data were processed in MS Excel, which included calculating error ranges. The quantification is based on a Fundamental Parameters algorithm designed by the manufacturer (Innov-X), with results given as wt% and ppm in elemental form. Raw chemical analyses are provided in Supplement Table S1.

3.4. Synchrotron Micro-XRF (SR-μXRF)

Preliminary assessment of the bulk chemistry obtained from the HHpXRF analyses showed some overlap between sources, which limited the possibility to discriminate unambiguously. Based on our analysis of a limited spectrum of trace elements (Mn, Cu, Co and Sb), we assumed that this pattern of strong overlap was repeated in the general element chemistry not accessible through conventional XRF. We chose at this stage an alternative route to determine micro-structures in the sample material. To evaluate these preliminary results and strengthen picrolite source discrimination, we opted for an additional set of analyses of a much higher microscopic resolution/spatial sensitivity. Our particular emphasis was on refining our preliminary bulk elemental analyses and investigating potential micro-structures that may have remained un-identified via HHpXRF but are likely to be key in achieving complete source discrimination.

The PUMA beamline at the SOLEIL synchrotron (Gif-sur-Yvette, France) is dedicated to the investigation of ancient materials and was developed in collaboration with the IPANEMA platform (Institut Photonique d'Analyse Non-destructive Européen des Matériaux Anciens) [13]. The PUMA (Photons Utilisés pour les Matériaux Anciens) beamline is a hard X-ray imaging beamline optimised for the scientific communities of the heritage sciences that allows for 2D imaging capabilities with a microscopic spatial resolution, applying several analytical techniques including X-ray fluorescence spectroscopy (XRF), on which this study is based. It generates photons using a 1.8 T wiggler insertion device with 8.98 keV critical energy. The beam is monochromatised with a Si(111) double crystal monochromator. A KB-mirror optic focalises the X-rays into a spot size of 5 μm diameter.

The picrolite samples were analysed using μXRF spectroscopy. Spot selection was based on distinct features noted on the samples after initial microscopy inspection at the IPANEMA laboratory. The samples were mounted with an angle of 45° to the incident beam, leading to an effective horizontal beam footprint of around 7 μm, and aligned with the video-microscope of the beamline. A beam energy of 13 keV was used to allow for the identification of the elements Ca, Ti, Cr, Fe, Co, Zn and As, at which the flux in the focal spot was around 1E10 photons/s. X-ray fluorescence spectra were recorded with a silicon drift detector (RaySpec Ltd., High Wycombe, UK) with a 100 mm^2 active area (on a chip 80 mm^2 collimated), a 450 μm-thick crystal and a 25 μm-thick Be window, installed at 90° from the incident beam. A cylindrically shaped aluminium collimator with 8 mm internal diameter and 10 mm length was used to reduce the spectral contribution of background scattering

and unwanted signals from the sample environment. Detection limits of 0.1–100 ppm for a 1 s measurement time and elements with an atomic number between 17 and 83 were obtained for geological, biological and glass sample matrices [23].

XRF cartographies were performed on an area typically of 1 mm^2 with 10 μm resolution and an acquisition time of 1 s using the so-called *flyscan* routine, in which the sample is moved continuously through the beam at a given speed and spectra are acquired over set time intervals, and were corrected for their encoder motor positions before visualisation of the data (see also [23]). The raw data are provided in Supplement Table S2.

3.5. Data Processing

The HHpXRF dataset was treated in a qualitative manner. In the cases where the concentration of the elements was either absent or unsystematically represented to all samples, the specific elements were excluded from the statistical treatment. Therefore, for the statistical manipulation of the picrolite specimens the following elements were used: Mg, Al, Si, Mn, Fe, Co, Cu and Sb. The extraction and inspection of SR-μXRF raw data was conducted using the SMAK data processing software package developed by Dr Sam Webb and available at SLAC [24]. For each elemental map, the number of counts for each element under investigation was extracted and normalised to 100%.

Subsequently, the processed datasets of both HHpXRF and SR-μXRF were further manipulated in Excel and statistically treated in MatLab. Principal components analysis (PCA) was employed to visualise and explore the relationships between the elements of north and south picrolite samples. The processed data were modified prior to running the PCA in order to remove the dilution effect introduced by non-measured elements and give approximately equal weight to all variables of interest. The standardisation followed here follows the notation by Baxter and Freestone [25]:

$$y_{ij} \leftarrow \left(x_{ij} - \overline{X_j}\right) / S_j \quad (1)$$

For the compositional matrix X made up of n cases and p variables, x_{ij} is the value for the jth variable of the ith case, X_J is the mean value of the jth variable and S_j is the sample standard deviation for the jth variable.

4. Results

4.1. HHpXRF Elemental Analysis

Multivariate statistical analysis of the dataset resulted in tentative source discrimination. Identification is based on the following major elements: Mg, Al, Si, Fe and, to a lesser degree on the trace elements, Mn and Cu (Figure 4). Principal component analysis showed that the first two eigenvectors explain 74% of the variance in the assemblage. There was a strong positive correlation of northern outcrops with Mn, Fe, Cu, Si and Mg on the first eigenvector and slightly negative correlations of Al on the first eigenvector. The second eigenvector was positively correlated with Al, Mn, Fe and Cu, but was not unambiguously able to separate the two source regions from each other. There were two clusters of samples which were plotted in discrete regions, giving good discrimination; however, six samples from the north ('agn' outcrops, and one 'bri' sample) and nine samples from the south ('pla' outcrops, two 'epi' samples, 'dex', 'eri' and 'geo') plotted close to each other, necessitating further analyses to increase source discrimination.

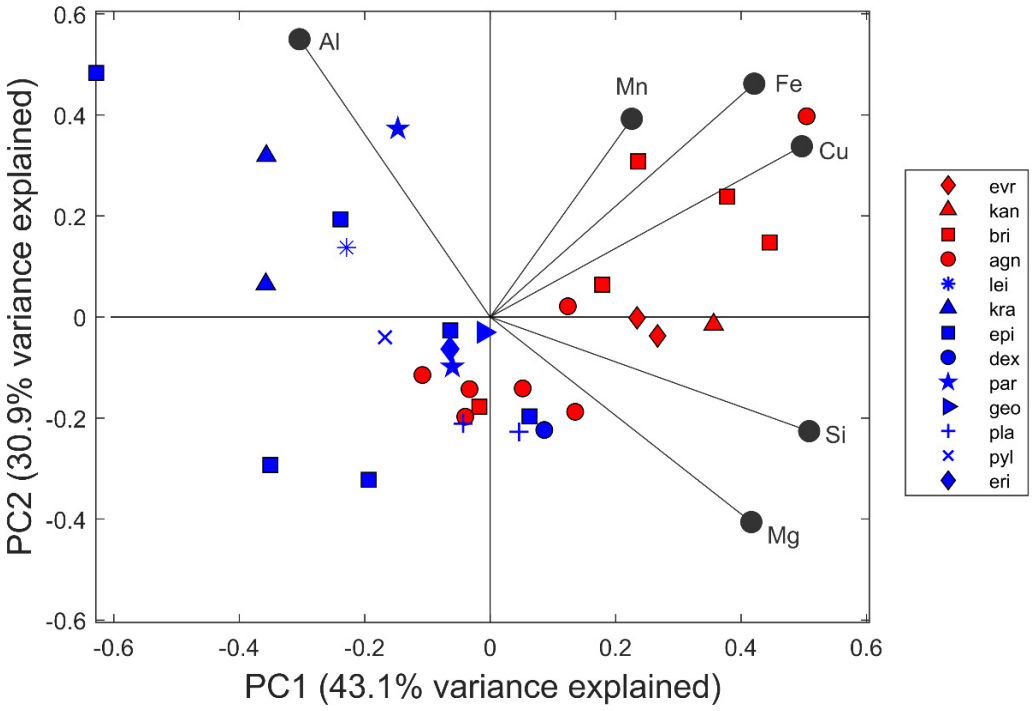

Figure 4. Principal component analysis (PCA) of picrolite elemental composition based on HHpXRF. Red symbols correspond to samples from the north; blue symbols represent samples from the south.

4.2. SR-μXRF Elemental Analysis

Principal component analysis (PCA) was applied to the concentrations of the elements Ca, Ti, Cr, Fe, Co, Zn and As. These elements were selected to maintain a comparative dataset with HHpXRF data (Supplement Table S1). The first two principal components explain 76.6% of the total variance (Figure 5). Component 1 accounts for 52.2% of the variance in the data and is characterised by high positive loadings of Ca, Ti, Cr, Zn and As. Component 2, which accounts for 24.4% of the total variance, separates strongly on second eigenvector where Fe is negative and Co positive. According to the multivariate analysis, SR-μXRF increases the source discrimination based on the chemical composition of the two major localities (i.e., north and south), in that only five samples from the south (one sample of each of the 'pyl', 'par' and 'epi', and 'pla' outcrops) overlap with samples from the north. Samples collected from the northern slopes of the Troodos Massif are tightly clustered, indicating a rather uniform elemental fingerprint. Conversely, picrolite specimens selected from southern locales display significant chemical variability along the elements of PC1. The sample collected from the southern locality Leivadi tou Pashia (lei 111.14) clusters far from the rest of the assemblage along the PC2 axis. The sample is characterised by elevated Fe and decreased Co content (G_{Fe} = 3.64, G_{Co} = 4.31; G_{Crit} = 2.76, a = 0.05) with respect to the other southern picrolite specimens, indicating that it should be treated as an outlier. The determination of sample lei 111.14 as an outlier has been established using Grubb's test for each element. The concentration of all elements within the assemblage follows an approximately normal distribution.

Bivariate plots (Figure 6) of elemental ratios normalised to iron (Fe) display clustering very similar to that of the samples in the PCA graph. The elements carrying the most structure in the assemblage are Ca, Zn, As and to a lesser extent Ti, Cr and Co. The chemical composition of the assemblage demonstrates that picrolite from the Karkotis River (north) is richer in Co, while elevated values of Ca, Cr, Zn and As describe the picrolite found following the course of Kouris River (south) (Table 2). Moreover, the analysis showed that a small number of picrolite samples from the south overlap with the north group, showing lower Ca, Zn, Cr and As values compared to the rest of the south group. The samples of 'epi' which overlapped in the PCA show slightly higher Cr and As values.

Higher Cr values are tentatively useful in separating 'par' samples from the northern sources. Calcium appears to be higher in one of the 'pla' outcrops, which might lead to a source discrimination. However, plotting the second set of 'pla' outcrops together with the northern source samples and a discrimination was not possible.

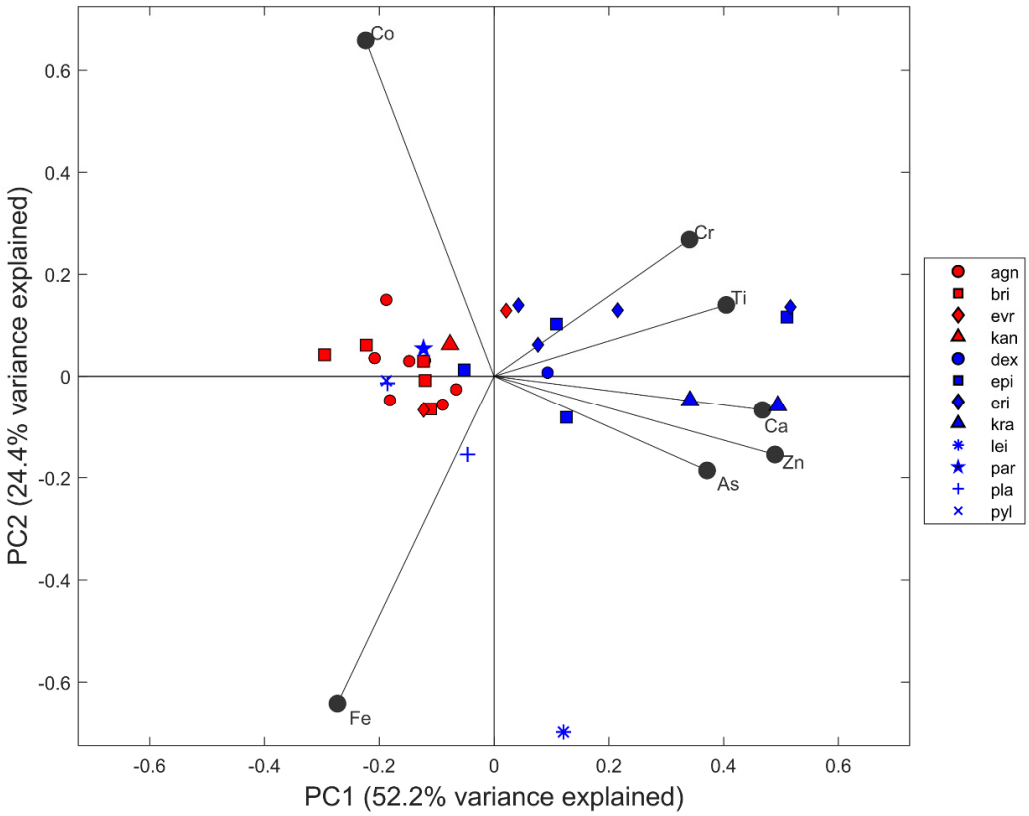

Figure 5. Principal component analysis (PCA) of picrolite elemental composition based on SR-*µXRF*. Red symbols correspond to samples from the north; blue symbols represent samples from the south.

Table 2. Average values of elemental ratios of picrolite normalised to iron (Fe). Note that all values are multiplied by 1000.

	Ca/Fe	Ti/Fe	Cr/Fe	Co/Fe	Zn/Fe	As/Fe
North	3.51	2.97	10.20	161.91	9.04	0.36
South	5.35	3.67	13.16	154.94	15.22	0.52

4.3. SR-µXRF Imaging

For additional analysis to identify possible pathways of source discrimination, SR-µXRF was applied to confirm the existence of micro-structural differences amongst our samples. As shown in Figure 7, a number of samples from the north group exhibited clearly distinguishable circular features (inclusions) of about 100 µm diameter within a largely homogenous matrix. These inclusions showed increased values of Fe, Co, Cr and Ti and have been tentatively identified as chromium-magnetite phenocrysts. These circular inclusions do not appear to be present in samples from the south group, which is overall characterised by a more homogenous matrix. Interestingly, the occurrence of these chromium-magnetite phenocrysts did not increase the overall Cr/Fe abundance of the bulk chemistry; however, they were useful for discriminating between sources—for example, the 'agn' and 'bri' outcrops that plotted together with the several southern samples in the HHpXRF plot.

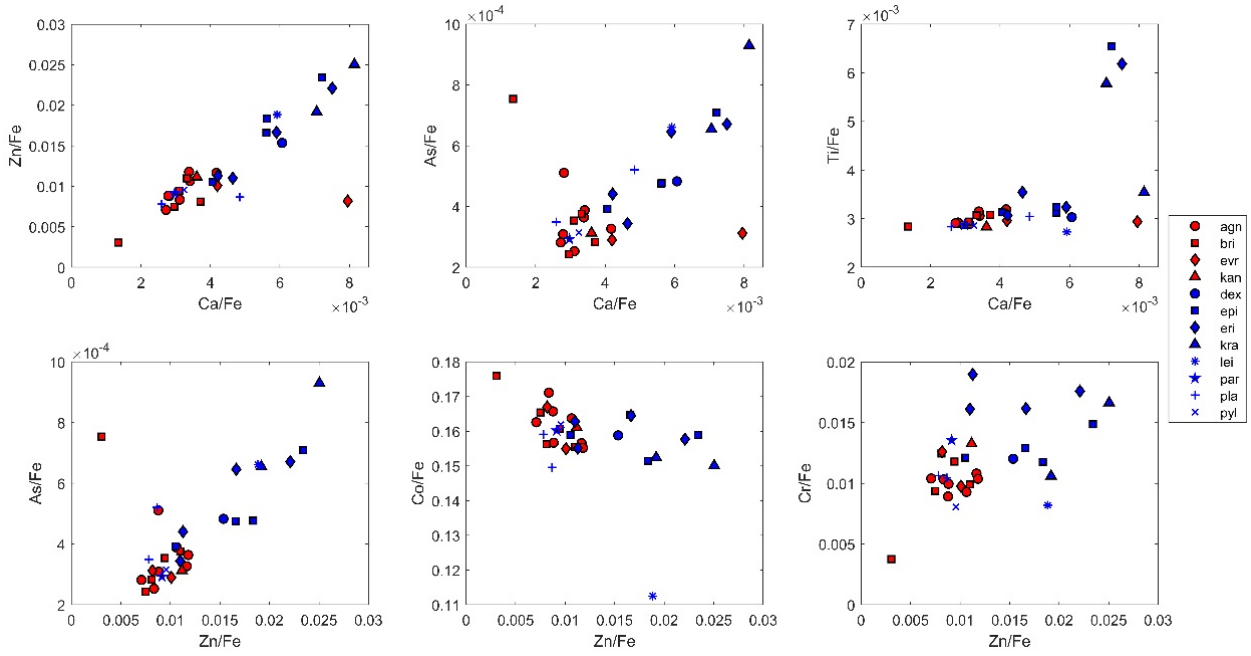

Figure 6. Bivariate plots of elemental ratios of picrolite normalised to iron (Fe). The chemical composition of the geological samples demonstrates that picrolite from the Karkotis River (north) is richer in Co, while elevated values of Ca, Cr, Zn and As describe the picrolite found following the course of Kouris River (south).

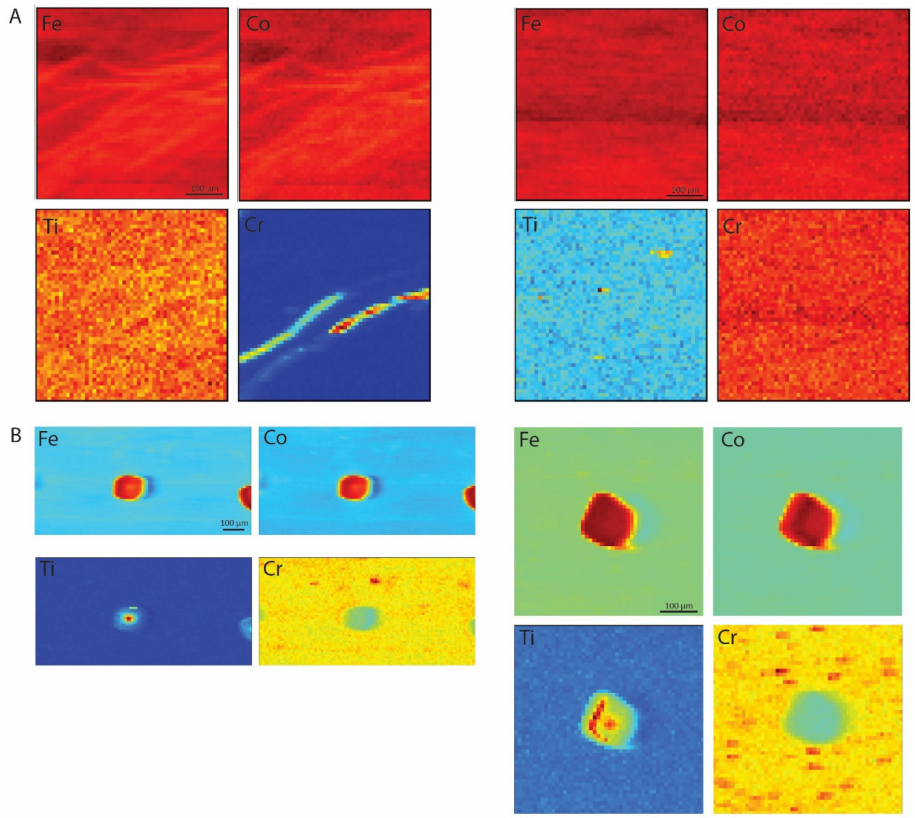

Figure 7. SR-μXRF images of picrolite samples (**A**) from the south (eri6-104.4, kra-113.14) featuring lamellar structures; (**B**) from the north group (agn-102.2, agn-102.4) depicting clearly distinguishable circular features (inclusions) of about 100 µm in diameter, tentatively identified as chromium-magnetite phenocrysts.

5. Discussion and Conclusions

The results obtained from the combined application of HHpXRF and SR-μXRF allowed us to successfully refine the basic characteristics of the elemental constituents of the picrolite raw material and capture key micro-structural differences between samples from two distinct source regions on the Troodos Massif in western Cyprus. Portable XRF is now an accepted method in archaeological research for the semi-quantitative and qualitative determination of elemental composition predominantly as it allows geochemical analyses to be non-destructive [26]. Non-destructive HHpXRF analysis showed the potential of discriminating the two source areas; however, several samples showed strong overlap in their respective geochemistry. The selected major elements Mg, Si, Mn and Fe and trace element abundances of Cu were particularly useful in achieving source discrimination. Unfortunately, two outcrops ('agn' and 'bri') were not unambiguously differentiated by HHpXRF alone.

High-resolution SR-μXRF analysis and imaging was employed to enhance source discrimination and applicability of non-destructive techniques. Multi-variate statistics of SR-μXRF element abundances showed a tight cluster of northern sources with a clearer separation of the two source regions using major elements of Ca, Fe and Ti with trace elements of Cr, As, Co and Zn. However, again several samples showed overlap. Additional high-resolution mapping of samples to identify possible micro-structures in the samples was successful in identifying several round inclusions in the samples from outcrops 'agn' and 'bri'. These inclusions were tentatively identified as chromium-magnetite phenocrysts and occurred only in the northern outcrops. The round inclusion had a diameter of approximately 100 µm diameter which is sufficiently large to be identified by analysis with a microscope.

Well-designed archaeometric studies can provide useful information in the study of ancient materials. The use of synchrotron radiation techniques to the study of archaeological and cultural heritage objects has undergone a steep increase over the past ten years or so. The methodology has been applied to a wide range of materials, including paintings, metals, glass and organics, such as bone, teeth and wood. Stone has rarely been the focus of such studies, particularly regarding the characterisation of raw materials for the manufacture of stone tools and other lithic objects. The results obtained from the application of SR-μXRF on picrolite samples add significant new data to the modest dataset of stone materials analysed via synchrotron radiation techniques. Moreover, the application of a state-of-the-art methodology with high spatial sensitivity (SR-μXRF) in combination with HHpXRF confirm the effectiveness of the latter in characterising the overall chemical composition of picrolite.

Distinguishing between different sources is crucial in filling significant research gaps in the broader field of archaeology, including raw material selectivity, human mobility, social communication and human–environment interactions. Within an Eastern Mediterranean context, determining the geological sources of picrolite on Cyprus opens up new avenues to address important questions on source utilisation in prehistoric Cyprus (e.g., [27]) and trace patterns of exploitation diachronically. Moreover, having a detailed elemental signature of the Cypriot picrolite sources opens up exciting new opportunities to investigate picrolite exchange routes within and, crucially, beyond the island boundaries. Hundreds of artefacts made of various 'green stones' are documented from the Levantine mainland (e.g., [28]) and remain, to date, unsourced. The possibility of at least some of these artefacts deriving from either of the Cypriot picrolite sources is now a distinct research opportunity, with exciting contributions to be made on key themes of global archaeological significance, such as island colonisation and island–mainland interactions.

Supplementary Materials: The following supporting information can be downloaded at: https://www.mdpi.com/article/10.3390/heritage5020037/s1, Table S1: HHpXRF data; Table S2: SR-μXRF data.

Author Contributions: Conceptualization, T.M. and M.T.; methodology, T.M., M.T., A.C., D.I., S.S., S.M.W. and C.R.; software, D.I., S.S. and S.M.W.; formal analysis, T.M., A.C., D.I., C.R. and S.S.; investigation, T.M., A.C., D.I., C.R., S.S. and Z.Z.; resources, M.T. and S.S.; writing—original draft preparation, T.M., C.R. and S.S.; review and editing, T.M., A.C., D.I., C.R., S.S., V.K., Z.Z., S.M.W. and M.T.; visualization, C.R., D.I. and T.M.; supervision, T.M., C.R., S.S. and S.M.W.; project administration, T.M.; funding acquisition, T.M. and V.K. All authors have read and agreed to the published version of the manuscript.

Funding: This work was funded by the Republic of Cyprus through the Research and Innovation Foundation (CULTURE/AWARD-YR/0418/0005) for the project Prehistoric Landscapes of Cyprus (PLACe, 2019–2021). We also wish to acknowledge financial support from the Access to Research Infrastructures activity in the H2020 Framework Programme of the EU (IPERION CH H2020-INFRAIA-2014-2015: Grant agreement no. 654028) for the beam time. Professor Kassianidou has also contributed funds from her research budget for this work.

Institutional Review Board Statement: Not applicable.

Informed Consent Statement: Not applicable.

Data Availability Statement: The data presented in this study are available upon request from the corresponding author. The data are not publicly available due to ongoing research.

Acknowledgments: We are grateful to the Geological Survey Department of the Republic of Cyprus for permits and to SOLEIL and IPANEMA for providing access to their facilities and the synchrotron team.

Conflicts of Interest: The authors declare no conflict of interest.

References

1. Peltenburg, E. *The Evolution of the Cypriot Cruciform Figurine. Report of the Department of Antiquities, Nicosia, Cyprus*; Getty Publications: Los Angeles, CA, USA, 1982.
2. Campo, A.L. *Anthropomorphic Representations in Prehistoric Cyprus: A Formal and Symbolic Analysis of Figurines, c. 3500–1800 BC. (Studies in Mediterranean Archaeology Pocket-Book 109)*; Paul Åström Förlag: Jonsered, Sweden, 1994.
3. Crewe, L.; Peltenburg, E.; Spanou, S. Contexts for cruciforms: Figurines of prehistoric Cyprus. *Antiquity* **2002**, *76*, 21–22. [CrossRef]
4. Simmons, A.H. Akrotiri-Aetokremnos (Cyprus) 20 years later: An assessment of its significance. *Eurasian Prehistory* **2013**, *10*, 139–156.
5. Simmons, A.H. Ais Giorkis: An unusual early Neolithic settlement in Cyprus. *J. Field Archaeol.* **2012**, *37*, 86–103. [CrossRef]
6. Peltenburg, E. Local exchange in prehistoric Cyprus: An initial assessment of picrolite. *Bull. Am. Sch. Orient. Res.* **1991**, *282–283*, 107–126. [CrossRef]
7. Moutsiou, T. Raw material circulation and the early holocene social landscape of Cyprus. In *Near Eastern Lithic Technologies on the Move. Interactions and Contexts in Neolithic Traditions, Proceedings of the 8th International Conference on PPN Chipped and Ground Stone Industries of the Near East, Nicosia, 23–27 November 2016 (Studies in Mediterranean archaeology Volume 150)*; Astruc, L., McCartney, C., Briois, F., Kassianidou, V., Eds.; Astrom Editions: Nicosia, Cyprus, 2019; pp. 119–132.
8. Cnudde, V.; Cnudde, J.P.; Dupuis, C.; Jacobs, P.J.S. X-ray micro-CT used for the localization of water repellents and consolidants inside natural building stones. *Mater. Charact.* **2004**, *53*, 259–271. [CrossRef]
9. Brunetti, A.; Princi, E.; Vicini, S.; Pincin, S.; Bidali, S.; Mariani, A. Visualization of monomer and polymer inside porous stones by using X-ray tomography. *Nucl. Instrum. Methods Phys. Res. Sect. B Beam Interact. Mater. At.* **2004**, *222*, 235–241. [CrossRef]
10. Mazel, V.; Richardin, P.; Debois, D.; Touboul, D.; Cotte, M.; Brunelle, A.; Walter, P.; Laprévote, O. The patinas of the Sogon-Tellem statuary: A new vision through physico-chemical analyses. *J. Cult. Herit.* **2008**, *9*, 347–353. [CrossRef]
11. Le Trong, E.; Rozenbaum, O.; Rouet, J.-L.; Bruand, A. A simple methodology to segment X-ray tomographic images of a multiphasic building stone. *Image Anal. Stereol.* **2008**, *27*, 175–182. [CrossRef]
12. Robertson, E.C.; Blyth, R. XANES investigation of the effects of heat treatment on an archaeological tool stone. In *Canadian Light Source 2008 Activity Report*; Canadian Light Source, Inc.: Saskatoon, SK, Canada, 2009.
13. Bertrand, L.; Languille, M.-A.; Cohen, S.X.; Robinet, L.; Gervais, C.; Leroy, S.; Bernard, D.; Le Pennec, E.; Josse, W.; Doucet, J.; et al. European research platform IPANEMA at the SOLEIL synchrotron for ancient and historical materials. *J. Synchrotron Radiat.* **2011**, *18*, 765–772. [CrossRef] [PubMed]
14. Bernardini, F.; Eichert, D.; Lenaz, D.; De Min, A.; Tuniz, C.; Velušček, A.; Montagnari Kokelj, E. Synchrotron FTIR microspectroscopy applied to the study of polished serpentinite artefacts: A non-destructive analytical approach. *Archaeometry* **2011**, *53*, 753–764. [CrossRef]

15. Xenophontos, C. Steatite vs. picrolite. P.59 in Early copper-work in Cyprus and the exploitation of picrolite: Evidence from the Lemba archaeological project, by E.J. Peltenburg. In *Early Metallurgy in Cyprus, 4000–4500 B.C.*; Muhly, J.D., Maddin, R., Karageorghis, V., Eds.; Pierides Foundation: Larnaka, Cyprus, 1981; pp. 41–62.
16. Whittaker, E.J.W.; Zussman, J. The characterization of serpentine minerals by X-ray diffraction. *Mineral. Mag. J. Mineral. Soc.* **1956**, *23*, 107–126. [CrossRef]
17. Wicks, F.J.; O'Hanley, D.S. Serpentine minerals: Structures and petrology. In *Hydrous Phyllosilicates: (Exclusive of Micas)*; Bailey, S.M.W., Ed.; De Gruyter: Boston, MA, USA, 1988; pp. 91–168. [CrossRef]
18. Chidester, A.; Albee, A.; Cady, W. *Petrology, Structure, and Genesis of the Asbestos-Bearing Ultramafic Rocks of the Belvidere Mountain Area in Vermont*; Geological Survey Professional Paper 1016; United States Government Printing Office: Washington, DC, USA, 1978.
19. Xenophontos, C. Picrolite, its nature, provenance, and possible distribution patterns in the Chalcolithic period of Cyprus. *Bull. Am. Sch. Orient. Res.* **1991**, *282–283*, 127–138. [CrossRef]
20. Dikaios, P. *Khirokitia: Final Report on the Excavation of a Neolithic Settlement in Cyprus on Behalf of the Department of Antiquities 1936–1946*; Oxford University Press: Oxford, UK, 1953.
21. Simmons, A.H. *Preliminary Report on Multidisciplinary Investigations at Neolithic Kholetria Ortos, Paphos District*; Report of the Department of Antiquities; Department of Antiquities: Nicosia, Cyprus, 1996; pp. 29–44.
22. Peltenburg, E. Picrolite, procurement, manufacture and use. In *Figurine Makers of Prehistoric Cyprus: Settlement and Cemeteries at Souskiou*; Peltenburg, E., Bolger, D., Crewe, L., Eds.; Oxbow Books: Oxford, UK, 2019; pp. 233–248.
23. Tack, P.; Bazi, B.; Vekemans, B.; Okbinoglu, T.; Van Maldeghem, F.; Goderis, S.; Schöder, S.; Vincze, L. Investigation of (micro-) meteoritic materials at the new hard X-ray imaging PUMA beamline for heritage sciences. *J. Synchrotron Radiat.* **2019**, *26*, 2033–2039. [CrossRef] [PubMed]
24. Webb, S.M. The MicroAnalysis Toolkit: X-ray Fluorescence Image Processing Software. *Am. Inst. Phys. Conf. Proc.* **2011**, *1365*, 196–199. [CrossRef]
25. Baxter, M.J.; Freestone, I.C. Log-ratio compositional data analysis in archaeometry. *Archaeometry* **2006**, *48*, 511–531. [CrossRef]
26. Bertrand, L.; Cotte, M.; Stampanoni, M.; Thoury, M.; Marone, F.; Schöder, S. Development and trends in synchrotron studies of ancient and historical materials. *Phys. Rep.* **2012**, *519*, 51–96. [CrossRef]
27. Cory-Lopez, E. Technological and material approaches to Cypriot Chalcolithic picrolite. In *Cypriot Material Culture Studies from Picrolite Carving to Proskynitaria Analysis, Proceedings of the 8th Annual Postgraduate Cypriot Archaeology Conference Held in Honour of the Memory of Paul Åström at the Vrije Universiteit Brussel (Belgium), 27–29 November 2008*; Jacobs, A., Cosyns, P., Eds.; Vubpress: Brussels, Belgium, 2015; pp. 25–45.
28. Bar-Yosef Mayer, D.; Porat, N. Green stone beads at the dawn of agriculture. *Proc. Natl. Acad. Sci. USA* **2008**, *105*, 8548–8551. [CrossRef]